nature physics

ARTICLES

PUBLISHED ONLINE: 15 JUNE 2015 | DOI: 10.1038/NPHYS3374

Percolation in real interdependent networks

Filippo Radicchi

The function of a real network depends not only on the reliability of its own components, but is affected also by the simultaneous operation of other real networks coupled with it. Whereas theoretical methods of direct applicability to real isolated networks exist, the frameworks developed so far in percolation theory for interdependent network layers are of little help in practical contexts, as they are suited only for special models in the limit of infinite size. Here, we introduce a set of heuristic equations that takes as inputs the adjacency matrices of the layers to draw the entire phase diagram for the interconnected network. We demonstrate that percolation transitions in interdependent networks can be understood by decomposing these systems into uncoupled graphs: the intersection among the layers, and the remainders of the layers. When the intersection dominates the remainders, an interconnected network undergoes a smooth percolation transition. Conversely, if the intersection is dominated by the contribution of the remainders, the transition becomes abrupt even in small networks. We provide examples of real systems that have developed interdependent networks sharing cores of 'high quality' edges to prevent catastrophic failures.

Percolation is among the most studied topics in statistical physics[1]. The model used to mimic percolation processes assumes the existence of an underlying network of arbitrary structure. Regular grids are traditionally considered to model percolation in materials[2,3]. Complex graphs are instead adopted in the analysis of spreading phenomena in social environments[4,5], or in robustness studies of technological and infrastructural systems[6–8]. Given a network, a configuration of the percolation model is generated assuming nodes present with probability p. For $p=0$, no nodes are present in the network, leading therefore to a disconnected configuration. For $p=1$, all nodes are present and within the same connected cluster. As p varies, the network undergoes a structural transition between these two extreme configurations. Usually, random percolation processes give rise to continuous phase transitions[9]. This means that the size of the largest cluster in the network, used as a proxy for the connectedness of the system, increases from the non-percolating to the percolating phases in a smooth fashion. Several theoretical approaches, that do not rely on the direct simulation of the model, are available for the analysis of percolation transitions in isolated real graphs. These include, among others, sets of heuristic equations to draw phase diagrams and estimate percolation thresholds[10–12], as well as effective protocols for the mitigation of malicious attacks[13–15].

The percolation transition may become discontinuous in a different model involving not just a single network, but a system composed of two or more interdependent graphs[16,17]. This is a very realistic scenario considering that many, if not all, real graphs are 'coupled' with other real networks. Examples can be found in several domains: social networks (for example, Facebook, Twitter) are coupled because they share the same actors[18]; multimodal transportation networks are composed of different layers (for example, bus, subway) that share the same locations[19,20]; the functioning of communication and power grid systems depend one on the other[16]. In the simplest case, one considers an interconnected system composed of only two network layers. The two layers have the same set of nodes, but not necessarily identical sets of edges (see Fig. 1). In the percolation model defined on this system, nodes are present with probability p. As p varies, the connectedness of the interdependent system is monitored through the size of the largest cluster of mutually connected nodes[16]. A cluster of mutually connected nodes is a set of vertices with the property that every node in the cluster has at least one neighbour belonging to that cluster in every layer. It has been proved that, in infinitely large interconnected systems composed of two uncorrelated random networks, the percolation transition is discontinuous[16,21,22]. However, this result has been shown not to apply to more general network models that account for degree correlations[23,24]. Unfortunately, all these theoretical approaches have been developed under two special, and unrealistic, assumptions. First, they hypothesize that network layers are generated according to graph models whose topology is not specified by a one-zero adjacency matrix, but a list of probabilities for pairs of nodes to be connected. Second, they apply only to the case of infinitely large systems. Real interdependent networks, on the other hand, have layers not compatible with network models, and finite size. In this paper, we introduce a novel set of heuristic equations able to describe percolation in interdependent networks under these two realistic conditions.

Our methodology builds on a recent theory developed for percolation in real isolated networks[10–12] (see Supplementary Information), and generalizes it to describe percolation transitions in two interdependent networks. Indicate with A and B the adjacency matrices of the two network layers. Each layer is given by an undirected and unweighted graph composed of N nodes. The structure of the graph in one of the two layers is encoded by the adjacency matrix A, a symmetric $N \times N$ matrix whose generic element $A_{ij}=1$, if vertices i and j share an edge, and $A_{ij}=0$, otherwise. The definition of the adjacency matrix B for the other layer is analogous. Without loss of generality, we assume that, when all nodes are present in the network, the graph is formed by a single mutually connected component. Let us consider an arbitrary value of the site occupation probability $p \in (0,1)$, and indicate with s_i the probability that the generic node i is part of the largest cluster of mutually connected nodes. The order parameter of the percolation transition is defined simply as the average of these probabilities over all nodes in the graph, that is,

$$P_\infty = \frac{1}{N}\sum_i s_i \qquad (1)$$

Center for Complex Networks and Systems Research, School of Informatics and Computing, Indiana University, Bloomington, Indiana 47408, USA.
e-mail: filiradi@indiana.edu

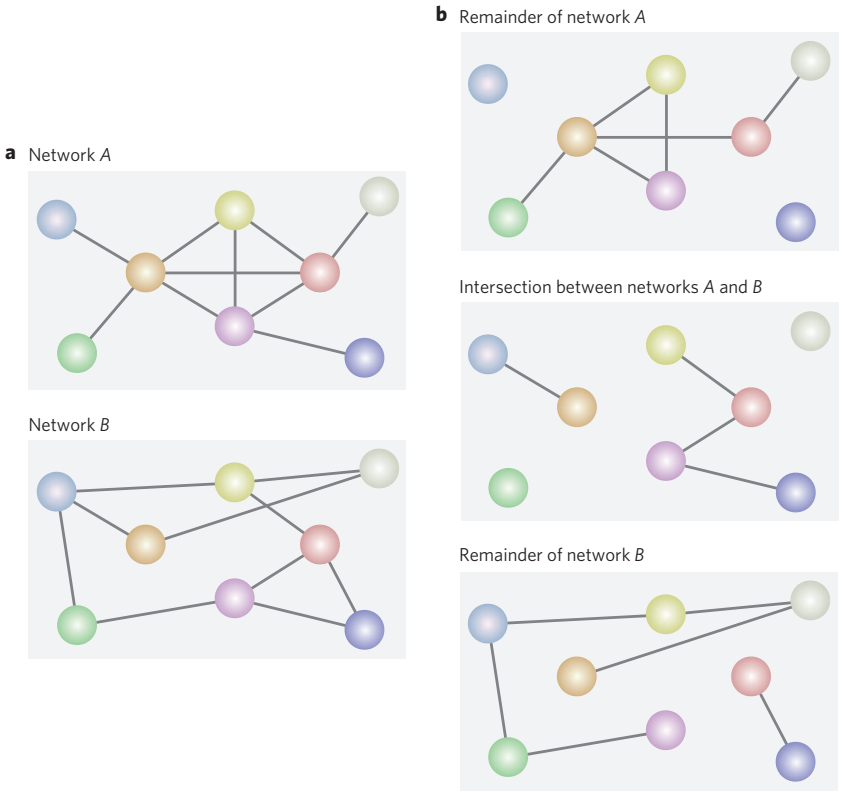

Figure 1 | Decomposition of interconnected networks into uncoupled graphs. a, Schematic example of two coupled networks *A* and *B*. In this representation, nodes of the same colour are one-to-one interdependent. **b**, In the percolation model, the interconnected system is equivalent to a set of three graphs that do not share any edge: the remainders of the network layers *A* and *B*, and their intersection.

Note that the variables s_i and the order parameter of equation (1) are functions of p, but, in the following, we omit this dependence for brevity of notation. Indicate respectively with $\mathcal{N}_i^A$ and $\mathcal{N}_i^B$ the sets of neighbours of vertex i on layers A and B. Then, define three disjoint sets of nodes: $\mathcal{AB}_i = \mathcal{N}_i^A \cap \mathcal{N}_i^B$ is the set of nodes that are neighbours of vertex i in both layers, $\mathcal{A}-\mathcal{B}_i = \mathcal{N}_i^A \setminus \mathcal{AB}_i$ is the set of nodes connected to vertex i only in layer A but not in B, and $\mathcal{B}-\mathcal{A}_i = \mathcal{N}_i^B \setminus \mathcal{AB}_i$ is the set of nodes that are neighbours of vertex i in layer B but not in A. Our first attempt to write the probability s_i that node i is in the largest mutually connected cluster of the system is given by the heuristic equation

$$s_i = p\,[S_{\mathcal{AB}_i} + (1 - S_{\mathcal{AB}_i})\, S_{\mathcal{A}-\mathcal{B}_i}\, S_{\mathcal{B}-\mathcal{A}_i}] \tag{2}$$

where $S_{\mathcal{X}} = 1 - \prod_{j\in\mathcal{X}}(1-s_j)$ is the probability that at least one of the nodes j in the set $\mathcal{X}$ is part of the largest cluster (for the empty set $\emptyset$, we have $S_\emptyset = 0$). Equation (2) states that, given that the vertex is occupied, the probability s_i for node i being part of the largest mutually connected cluster is given by the sum of two contributions: first, the probability to be connected to the largest cluster thanks to at least one vertex connected to i in both layers; second, if the latter condition is not true, the probability that node i is connected to the largest cluster through at least one node k in layer A and one node ℓ in layer B, with $k \neq \ell$. Note that, if the network layers are identical, then equation (2) correctly reduces to the equation valid for isolated networks (see Supplementary Information). In other words, one can split the set of edges in the system into three different subsets, and then construct three different graphs on the basis of this unique division (see Fig. 1): the intersection graph with adjacency matrix given by the Hadamard product of the matrices A and B [that is, the (i,j)th element of the adjacency matrix is $A_{ij}B_{ij}$]; the remnant of network A, where the edge between nodes i and j is present only if $A_{ij}(1-B_{ij}) = 1$; and the remainder of graph B, whose (i,j)th adjacency matrix element equals $B_{ij}(1-A_{ij})$. If we define $u_i = \ln(1-s_i)$, we can write $S_{\mathcal{AB}_i} = 1 - \exp\,[\sum_j A_{ij}B_{ij}u_j]$, $S_{\mathcal{A}-\mathcal{B}_i} = 1 - \exp\,[\sum_j A_{ij}(1-B_{ij})u_j]$ and $S_{\mathcal{B}-\mathcal{A}_i} = 1 - \exp\,[\sum_j B_{ij}(1-A_{ij})u_j]$. Thus, the numerical solution of equation (2) can be obtained in a certain number of iterations, each having a computational complexity that grows as the number of edges present in the denser layer. In the linear approximation, the transition is determined only by the contribution of the intersection graph. So, if the intersection 'dominates' the remainders, the transition is smooth, and the percolation threshold is approximated by $1/\lambda_{\mathrm{I}}$, where λ_{I} is the largest eigenvalue of the adjacency matrix of the intersection graph (see Supplementary Information).

The most serious limitation of equation (2) is to introduce a positive feedback among probabilities. An increment in the probability s_i produces an increase in the probabilities s_j of the neighbours, which in turn causes an increment in the probability s_i, and so on. The same exact problem arises in the study of percolation on isolated networks, and represents the basic difference between heuristic equations that lead to the same estimate for the percolation threshold as the one provided by Bollobás *et al.* in dense graphs[10], and the heuristic approaches by Karrer *et al.*[11] and Hamilton and Pryadko[12] in sparse tree-like graphs (see Supplementary Information). To avoid the presence of self-reinforcement mechanisms in equation (2), we introduce another system of heuristic equations, according to which s_i obeys

$$s_i = p\,[R_{\mathcal{AB}_i} + (1 - R_{\mathcal{AB}_i})\, R_{\mathcal{A}-\mathcal{B}_i}\, R_{\mathcal{B}-\mathcal{A}_i}] \tag{3}$$

where $R_{\mathcal{X}_i} = 1 - \prod_{j\in\mathcal{X}}(1-r_{i\to j})$, and the three sets $\mathcal{AB}_i$, $\mathcal{A}-\mathcal{B}_i$ and $\mathcal{B}-\mathcal{A}_i$ are defined as above. Here, $r_{i\to j}$ stands for the probability that node j is part of the largest cluster of mutually connected nodes,

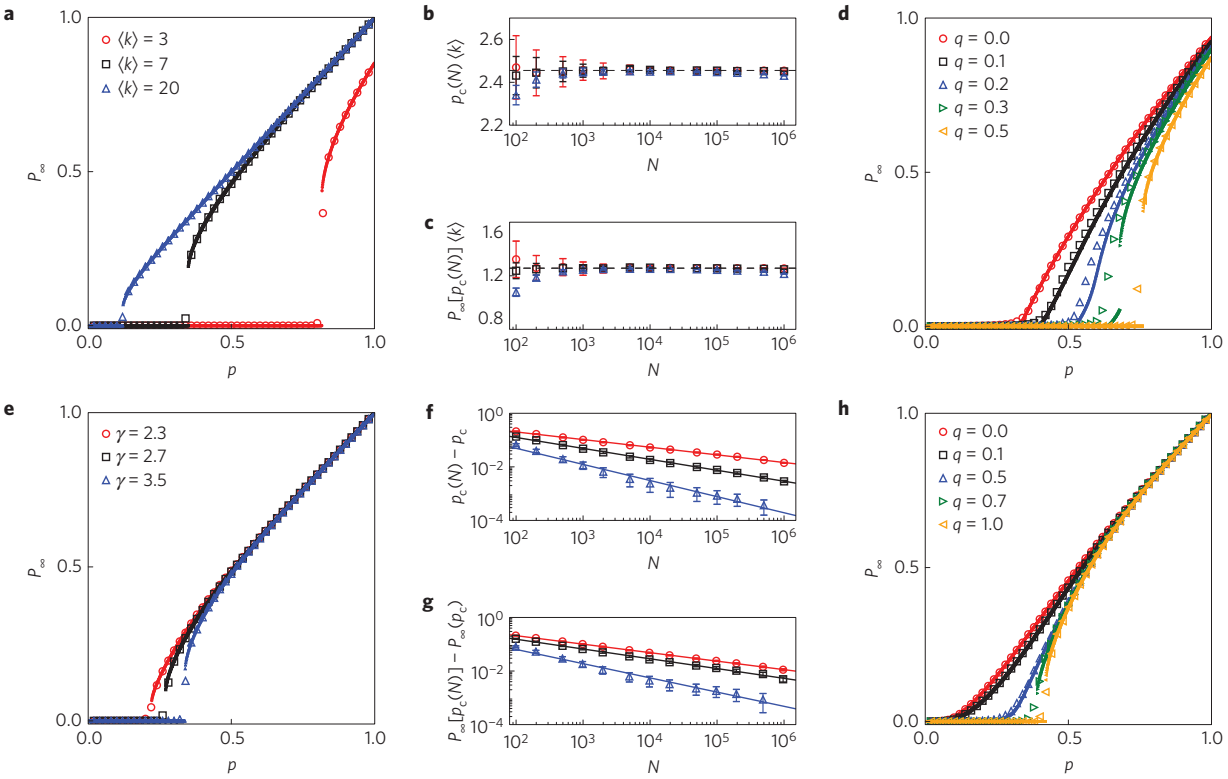

Figure 2 | Percolation transition in artificial interconnected networks. a, Percolation diagrams for interdependent Erdős–Rényi (ER) graphs with average degree $\langle k\rangle$. We compare results of numerical simulations (large symbols) with the solutions of our equations (small symbols). Results are obtained on a single instance of the network model, where both layers have size $N=10^4$. Different colours and symbols refer to different values of the average degree $\langle k\rangle$. **b**,**c**, Finite-size scaling analysis for coupled ER models. For a given size N of the network, we generate several instances of the model, and compute $p_c(N)$ (**b**) and $P_\infty[p_c(N)]$ (**c**) using the numerical solution of our equations (see Supplementary Information). Both quantities are multiplied by the average degree $\langle k\rangle$. Points refer to average values obtained over several realizations of the graph model and error bars stand for standard deviations. We use the same symbols and colours as those of **a**. Results are compared with $p_c\langle k\rangle=2.4554$ and $P_\infty(p_c)\langle k\rangle=1.2564$ (dashed black lines), as predicted by Buldyrev *et al.* in the limit $N\to\infty$ (ref. 16). **d**, We generate a single ER graph with $N=10^4$ and $\langle k\rangle=3$, and use it as structure for both layers. We then exchange, with probability q, the label of every node of layer A with a randomly selected vertex. Results of numerical simulations (large symbols) are compared with the solutions of our equations (small symbols). **e**, Percolation diagrams for single instances of interconnected scale-free networks. Each layer is obtained by randomly connecting vertices whose degrees obey the distribution $P(k)\sim k^{-\gamma}$, if $k\in[k_{\min},\sqrt{N}]$, and $P(k)=0$, otherwise. Here, $N=10^4$ and $k_{\min}=5$. Results of numerical simulations (large symbols) are compared with the solutions of our equations (small symbols). **f**,**g**, Finite-size scaling analysis for coupled scale-free networks ($k_{\min}=3$). As the size N of the network grows, the pseudo-critical threshold $p_c(N)$ gets closer to the critical threshold p_c in a power-law fashion (**f**). Similar scaling hypothesis are tested for $P_\infty[p_c(N)]$ (**g**). Points indicate average values obtained, using the numerical solution of our equations (see Supplementary Information), over at least ten independent realizations of the network model. Error bars quantify instead the standard deviation of the measures across different realizations. For any value of the degree exponent γ, we find that the asymptotic values p_c and $P_\infty(p_c)$ are strictly larger than zero (see Supplementary Information). **h**, We generate a graph with $N=10^4$ nodes, and degrees extracted from a power-law distribution ($\gamma=2.5$, $k_{\min}=3$). We use this network as structure for both layers. We then exchange, with probability q, the label of every node of layer A with a randomly selected vertex. Results of numerical simulations (large symbols) are compared with the solutions of our equations (small symbols).

disregarding whether vertex i belongs to it or not. Although this quantity can be defined for any pair of nodes, only contributions given by adjacent vertices play a role in equation (3). We can think of $r_{i\to j}$ as one of the $2E$ components of a vector $\mathbf{r}$. In the definition of $\mathbf{r}$, every edge (i,j) in the graph is responsible for two entries—namely, $r_{i\to j}$ and $r_{j\to i}$. For consistency, the probability $r_{i\to j}$ is described by the following heuristic equation

$$r_{i\to j}=p\left[R_{\mathcal{AB}_j\setminus\{i\}}+(1-R_{\mathcal{AB}_j\setminus\{i\}})\,R_{\mathcal{A}-\mathcal{B}_j\setminus\{i\}}\,R_{\mathcal{B}-\mathcal{A}_j\setminus\{i\}}\right] \qquad (4)$$

The products on the r.h.s. of equation (4) run over all neighbours of node j, excluding vertex i. If the network layers are identical, then equations (3) and (4) reduce to the equations valid for an isolated network (see Supplementary Information). If we indicate with $\mathbf{r}^{(AB)}$ the vector whose components are generated by edges present in the intersection graph, $\mathbf{w}^{(AB)}$ the vector with entries of the type $w^{(AB)}_{i\to j}=\ln(1-r^{(AB)}_{i\to j})$, and $M^{(AB)}$ the non-backtracking matrix[25,26] of the intersection graph, we can write $R_{\mathcal{AB}_j\setminus\{i\}}=1-\exp\left[\sum_{k\to\ell}M^{(AB)}_{i\to j,k\to\ell}\,w^{(AB)}_{k\to\ell}\right]$. In a similar spirit, we can also write $R_{\mathcal{A}-\mathcal{B}_j\setminus\{i\}}=1-\exp\left[\sum_{k\to\ell}M^{(A-B)}_{i\to j,k\to\ell}\,w^{(A-B)}_{k\to\ell}\right]$ and $R_{\mathcal{B}-\mathcal{A}_j\setminus\{i\}}=1-\exp\left[\sum_{k\to\ell}M^{(B-A)}_{i\to j,k\to\ell}\,w^{(B-A)}_{k\to\ell}\right]$, where these equations are respectively valid only for edges that belong to either layer A or B. Our equations generalize the use of the non-backtracking matrix to study percolation from isolated to interdependent networks. Whereas the role of the intersection graph in percolation on interdependent graph models of infinite size has been recently considered in some works[27–29], we are not aware of existing theoretical approaches of direct applicability to arbitrary finite-size networks. In the linear approximation, the transition is determined only by the contribution of the intersection graph, and the problem becomes equivalent to the one valid for isolated networks[11,12]: the transition is smooth, and the percolation threshold is given by $1/\mu_1$, with μ_1 being the largest eigenvalue of the non-backtracking matrix of the intersection graph (see Supplementary Information). Note that

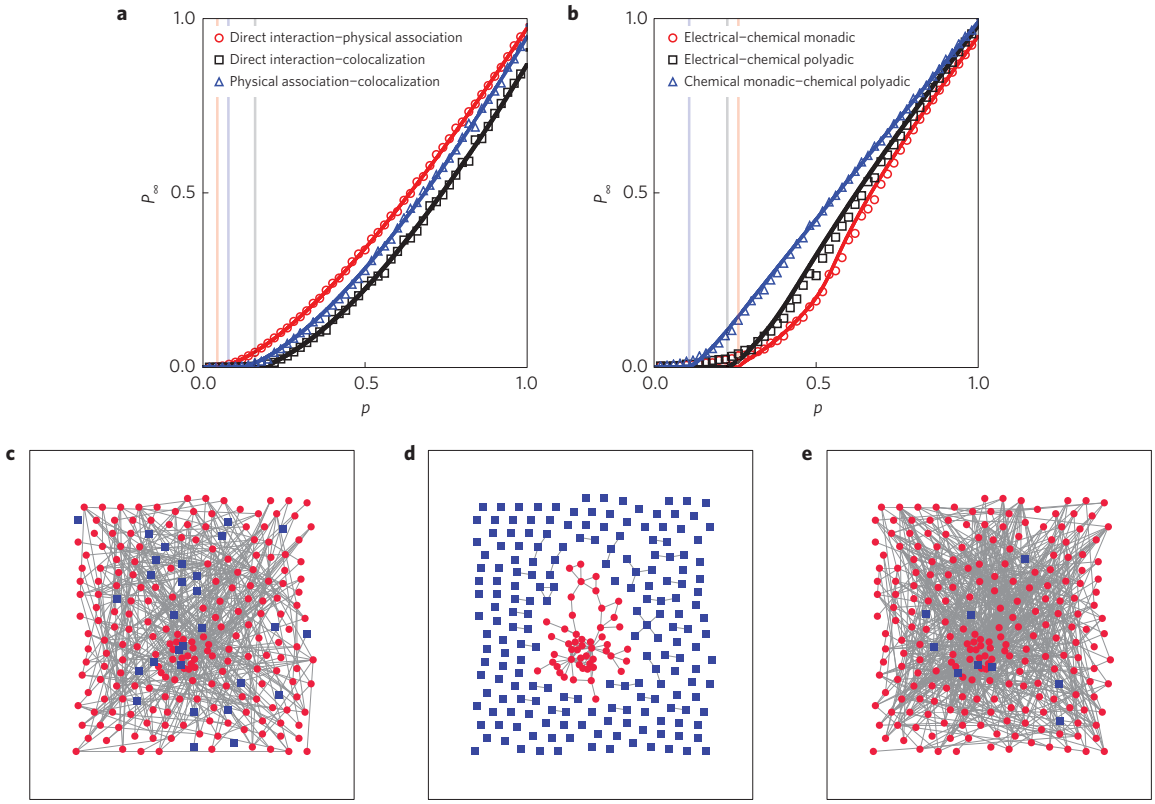

Figure 3 | Percolation transition in interdependent biological networks. a, Phase diagram for the multi-layer *H. sapiens* protein interaction network[36,37]. Edges in different layers represent diverse types of connections among proteins: direct interaction, physical association and co-localization. When analysing a multiplex with two of these layers, we restrict our attention only to the set of nodes present in both layers. For each of the three systems formed by two interconnected networks that we can generate with this data, we draw the percolation diagram by means of numerical simulations (large symbols) and numerical solution of our equations (small symbols). Vertical shaded lines stand for $1/\mu_1$, with μ_1 being the largest eigenvalue of the non-backtracking matrix of the intersection graph. **b**, Phase diagram for the multi-layer network of the *C. elegans* connectome[37]. Edges in different layers represent different types of synaptic junctions among the neurons: electrical, chemical monadic and chemical polyadic. Vertical shaded lines stand for $1/\mu_1$. **c**–**e**, Decomposition of the multi-layer *C. elegans* connectome. **c**, Remnant of the layer corresponding to electrical junctions. **d**, Intersection among the layers corresponding to electrical and chemical monadic interactions. **e**, Remainder of the layer corresponding to chemical monadic junctions. In panels **c**–**e**, nodes belonging to the largest connected component are represented with red circles. All other nodes are represented with blue squares. Although the remainders contain the vast majority of edges in the system, the largest component in the intersection graph (**d**) is characterized by a core of nodes and edges compact enough to prevent an abrupt percolation transition.

the interesting physics for percolation on interconnected networks becomes apparent only if the nonlinear terms of equations (3) and (4) are not neglected. Owing to the nonlinearity of the problem, we can rely only on the numerical solution of the equations. This can be obtained by iteration in a relatively fast way, because every iteration has a computational complexity that scales linearly with the total number of edges E, and the computational time τ required to draw the entire diagram for a given network scales as $\tau \sim E\ln(E)$ (see Supplementary Information). We stress that the solution of the equations provides, at cost of working in the locally tree-like approximation, the entire percolation diagram of a given interconnected network over an infinite number of realizations of the percolation model without the need to run any simulation. Tree-based approximations clearly do not apply to regular lattices, but allow effective methods also in many real networks that are not locally tree-like[11,30]. The same solution obtained from our equations can be used to describe not only site but also bond percolation. The order parameters of the two models differ only by a multiplicative factor, so we can solve one model using the other (see Supplementary Information). We believe that this represents a great achievement, although efficient algorithms to simulate percolation processes—either site or bond—in interdependent networks are already available on the market[31,32].

Phase diagrams obtained through the numerical solution of equations (3) and (4) reproduce the results of numerical simulations very accurately. In Fig. 2a, we consider systems composed of two independent Erdős–Rényi network models with average degree $\langle k\rangle$. A fundamental feature that the diagrams reveal is the presence of a sudden jump in the order parameter P_∞ at a certain threshold p_c, in the sense that the left- and right-hand limits of the function P_∞ are different at $p = p_c$. Our equations predict the presence of a point discontinuity for P_∞ in networks of finite size. This jump is due to the nonlinear terms of equations (3) and (4). A similar nonlinearity, and resulting discontinuity, arises also in equations associated with cores in random graphs[33]. As the linearization of equations (3) and (4) is not useful in revealing the eventual presence of a discontinuity in P_∞, the identification of p_c cannot be reduced to the solution of an eigenvalue problem, as in the case of smooth transitions in isolated networks (see Supplementary Information). Note that a discontinuity for P_∞ in finite-size networks may not correspond to a true discontinuous phase transition, unless a non-vanishing jump persists also in the limit of infinitely large networks[34]. The latter is what we observe in our finite-size scaling analyses of Fig. 2b,c. As the system grows in size, the location of the critical point p_c and the height of the jump $P_\infty(p_c)$ stabilize to values already predicted for this type of graph model in the

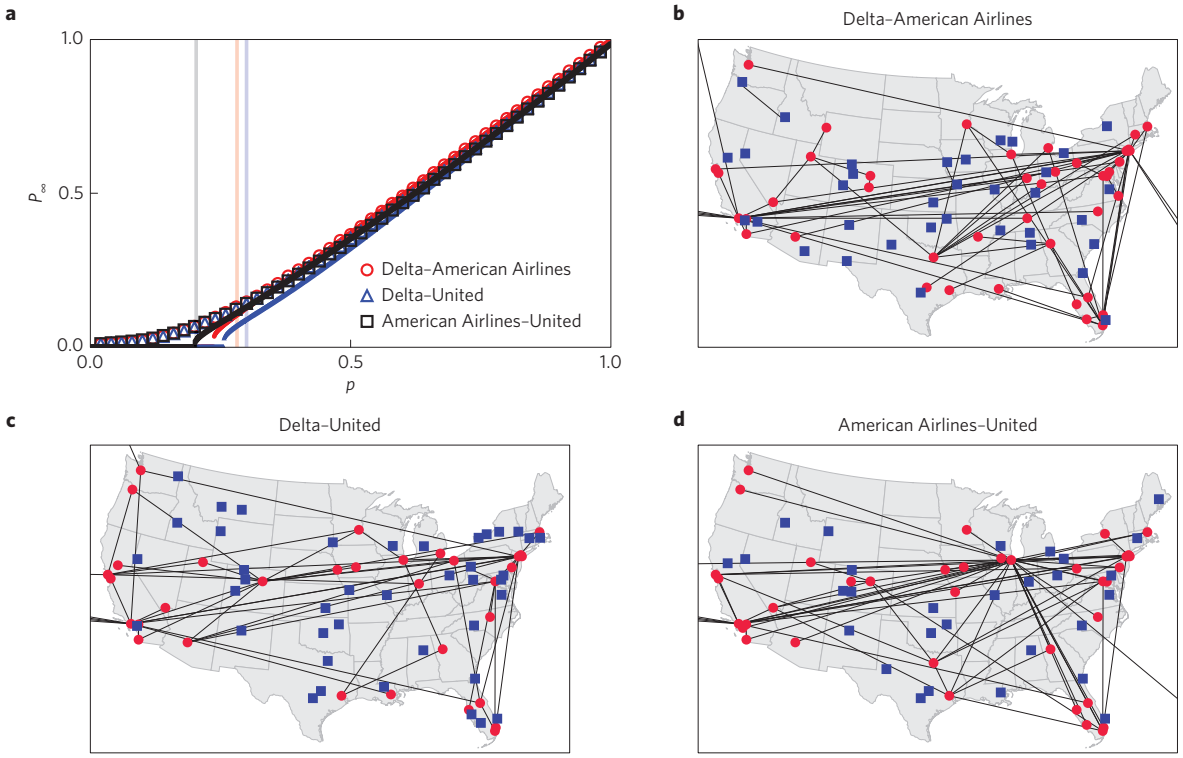

Figure 4 | Percolation transition in interconnected transportation networks. a, Red points refer to results obtained on the interdependent network whose layers are given by Delta and American Airlines routes, respectively. We consider only US domestic flights operated in January 2014 (ref. 40), and construct an interconnected network where airports are nodes, and connections on the layers are determined by the existence of at least one flight between the two locations. In the percolation diagram, large symbols are results of numerical simulations, whereas small symbols represent the solutions of our equations. We perform the same analysis also for the combination of flights Delta—United (blue) and American Airlines—United (black). Vertical shaded lines indicate $1/\mu_1$—that is, the predicted threshold values for percolation on the intersection graphs. **b**–**d**, Intersection graphs for the systems analysed in **a**. In the various network visualizations, nodes belonging to the largest connected component are represented with red circles. All other nodes are instead represented with blue squares. Major airports and connections among them constitute the structural cores that make these networks robust against abrupt percolation transitions.

limit of infinite size[16,21,22]. We argue that P_∞ exhibits a sudden jump only if the contribution of the remainders dominates the importance of the intersection. This condition is certainly verified in interdependent Erdős–Rényi graphs, where the intersection is composed of a very small number of edges, roughly equal to $\langle k\rangle^2/2$, whereas the number of edges in each of the remnants is proportional to $\langle k\rangle N/2$. Our intuition is fully supported by the results of Fig. 2d. Here, we control for the weight of the intersection with respect to those of the remnants in a simple fashion[35]. The two layers have the same network structure. Labels of interdependent nodes are, however, shuffled with probability q. For small q values, P_∞ varies in a smooth fashion over the entire phase diagram. For sufficiently large q values, P_∞ exhibits a discontinuous behaviour. For intermediate values of q, the jump does not start off from zero, but the discontinuity is anticipated by a smooth increase. Finite-size scaling analyses confirm that, even in this regime, $P_\infty(p_c)$ does decrease to zero as the size of the system grows (see Supplementary Information). This model provides further insights. We find that the percolation transition changes its nature—from continuous to discontinuous—approximately when the largest eigenvalue μ_1 of the non-backtracking matrix of the largest component of the intersection graph becomes comparable to the smallest among the largest eigenvalues of the same matrices defined for the remainders, namely $\mu_{A,B}$. These considerations are valid also for other homogeneous networks, such as coupled regular graphs (see Supplementary Information).

Next, we consider the case of network layers given by scale-free random graphs. A jump for P_∞ is visible in finite-size networks if the layers are sufficiently sparse and generated in an independent manner, so that only the remainders are present (Fig. 2e). Finite-size scaling analyses allow one to extrapolate, for networks of infinite size, non-vanishing asymptotic values for p_c (Fig. 2f) and $P_\infty(p_c)$ (Fig. 2g). The transition in finite networks can be tuned from smooth to abrupt by randomly relabelling, with probability q, nodes in one of the two layers, despite the layers having identical structure (Fig. 2h). If we observe P_∞ as a function of q for different system sizes, we note, however, a fundamental difference with respect to the case of homogeneous graphs. The change in the nature of the transition is not delimited by the condition $\mu_1-\mu_{A,B}=0$. This fact can be explained by considering that hub-to-hub edges play a central role in percolation processes[15]. Until q becomes large enough to allow a sufficient number of hubs to be relabelled, the percolation transition cannot become abrupt (see Supplementary Information). Thus, in heterogeneous graphs, the nature of the transition is not determined by the number of edges shared across layers, but rather their 'quality'.

Similar considerations may serve to explain why real interdependent networks seem not to experience catastrophic failures[24]. In Fig. 3, we draw the percolation diagrams for two interconnected systems of interest in the biological sciences: the *H. sapiens* protein interaction network[36,37], and the *C. elegans* connectome[37]. These interconnected systems undergo smooth percolation transitions, perfectly reproduced by our equations. Connections in the intersection graph account for less than 10% in five out of the six interdependent networks analysed (see Supplementary Information). Therefore, it seems that these

organisms have developed interconnected networks sharing a core of 'high quality' edges to prevent catastrophic failures. This observation can be more quantitatively supported by the fact that the P_∞ starts to smoothly increase from zero for $p \simeq 1/\mu_1$, as the linear expansion of the equations would predict (see Supplementary Information). The same properties seem to characterize also the multi-layer air transportation network within the US (Fig. 4)[38,39]. Although a small discontinuity is visible in the solution of our heuristic equations, the height of the jump is not as marked as observed in random uncorrelated graphs. Major airports all belong to the largest connected component of the intersection graph, and their connections constitute a set of 'high quality' edges that avoid truly catastrophic changes in the connectedness of the entire interdependent system.

In summary, we introduced a novel set of equations able to fully characterize percolation phase diagrams in finite-size interdependent networks. The framework helps in providing an independent method, being orthogonal to most of other approaches available on the market, to identify cores of quality links able to prevent catastrophic failures in real systems. Whereas the networks analysed here indicate that quality links mainly correspond to hub-to-hub edges, thus confirming previously established results[14,15,23,24], we do not exclude that our framework may be able to identify, in other real systems, cores of 'high quality' edges with completely different features. Also, we speculate that our equations, with suitable modifications accounting for node or edge attributes, may be used for the optimization of network quality functions other than robustness.

Received 13 January 2015; accepted 21 May 2015;
published online 15 June 2015

References

1. Stauffer, D. & Aharony, A. *Introduction to Percolation Theory* (Taylor and Francis, 1991).
2. Kirkpatrick, S. Percolation and conduction. *Rev. Mod. Phys.* **45,** 574–588 (1973).
3. Berkowitz, B. Analysis of fracture network connectivity using percolation theory. *Math. Geol.* **27,** 467–483 (1995).
4. Pastor-Satorras, R. & Vespignani, A. Epidemic spreading in scale-free networks. *Phys. Rev. Lett.* **86,** 3200–3203 (2001).
5. Newman, M. E. Spread of epidemic disease on networks. *Phys. Rev. E* **66,** 016128 (2002).
6. Albert, R., Jeong, H. & Barabási, A-L. Error and attack tolerance of complex networks. *Nature* **406,** 378–382 (2000).
7. Cohen, R., Erez, K., Ben-Avraham, D. & Havlin, S. Resilience of the Internet to random breakdowns. *Phys. Rev. Lett.* **85,** 4626–4628 (2000).
8. Callaway, D. S., Newman, M. E., Strogatz, S. H. & Watts, D. J. Network robustness and fragility: Percolation on random graphs. *Phys. Rev. Lett.* **85,** 5468–5471 (2000).
9. Dorogovtsev, S. N., Goltsev, A. V. & Mendes, J. F. Critical phenomena in complex networks. *Rev. Mod. Phys.* **80,** 1275–1335 (2008).
10. Bollobás, B. *et al.* Percolation on dense graph sequences. *Ann. Prob.* **38,** 150–183 (2010).
11. Karrer, B., Newman, M. E. J. & Zdeborová, L. Percolation on sparse networks. *Phys. Rev. Lett.* **113,** 208702 (2014).
12. Hamilton, K. E. & Pryadko, L. P. Tight lower bound for percolation threshold on an infinite graph. *Phys. Rev. Lett.* **113,** 208701 (2014).
13. Cohen, R., Havlin, S. & Ben-Avraham, D. Efficient immunization strategies for computer networks and populations. *Phys. Rev. Lett.* **91,** 247901 (2003).
14. Moreira, A. A., Andrade, J. S. Jr, Herrmann, H. J. & Indekeu, J. O. How to make a fragile network robust and vice versa. *Phys. Rev. Lett.* **102,** 018701 (2009).
15. Schneider, C. M., Moreira, A. A., Andrade, J. S., Havlin, S. & Herrmann, H. J. Mitigation of malicious attacks on networks. *Proc. Natl Acad. Sci. USA* **108,** 3838–3841 (2011).
16. Buldyrev, S. V., Parshani, R., Paul, G., Stanley, H. E. & Havlin, S. Catastrophic cascade of failures in interdependent networks. *Nature* **464,** 1025–1028 (2010).
17. Radicchi, F. & Arenas, A. Abrupt transition in the structural formation of interconnected networks. *Nature Phys.* **9,** 717–720 (2013).
18. Szell, M., Lambiotte, R. & Thurner, S. Multirelational organization of large-scale social networks in an online world. *Proc. Natl Acad. Sci. USA* **107,** 13636–13641 (2010).
19. Barthélemy, M. Spatial networks. *Phys. Rep.* **499,** 1–101 (2011).
20. De Domenico, M., Solé-Ribalta, A., Gómez, S. & Arenas, A. Navigability of interconnected networks under random failures. *Proc. Natl Acad. Sci. USA* **111,** 8351–8356 (2014).
21. Gao, J., Buldyrev, S. V., Stanley, H. E. & Havlin, S. Networks formed from interdependent networks. *Nature Phys.* **8,** 40–48 (2012).
22. Son, S-W., Bizhani, G., Christensen, C., Grassberger, P. & Paczuski, M. Percolation theory on interdependent networks based on epidemic spreading. *Europhys. Lett.* **97,** 16006 (2012).
23. Radicchi, F. Driving interconnected networks to supercriticality. *Phys. Rev. X* **4,** 021014 (2014).
24. Reis, S. D. *et al.* Avoiding catastrophic failure in correlated networks of networks. *Nature Phys.* **10,** 762–767 (2014).
25. Hashimoto, K-i. *Automorphic Forms and Geometry of Arithmetic Varieties* 211–280 (Kinokuniya Company Ltd., 1989).
26. Krzakala, F. *et al.* Spectral redemption in clustering sparse networks. *Proc. Natl Acad. Sci. USA* **110,** 20935–20940 (2013).
27. Hu, Y. *et al.* Percolation of interdependent networks with intersimilarity. *Phys. Rev. E* **88,** 052805 (2013).
28. Cellai, D., López, E., Zhou, J., Gleeson, J. P. & Bianconi, G. Percolation in multiplex networks with overlap. *Phys. Rev. E* **88,** 052811 (2013).
29. Min, B., Lee, S., Lee, K-M. & Goh, K-I. Link overlap, viability, and mutual percolation in multiplex networks. *Chaos Solitons Fractals* **72,** 49–58 (2015).
30. Melnik, S., Hackett, A., Porter, M. A., Mucha, P. J. & Gleeson, J. P. The unreasonable effectiveness of tree-based theory for networks with clustering. *Phys. Rev. E* **83,** 036112 (2011).
31. Schneider, C. M., Araújo, N. A. M. & Herrmann, H. J. Algorithm to determine the percolation largest component in interconnected networks. *Phys. Rev. E* **87,** 043302 (2013).
32. Hwang, S., Choi, S., Lee, D. & Kahng, B. Efficient algorithm to compute mutually connected components in interdependent networks. *Phys. Rev. E* **91,** 022814 (2015).
33. Pittel, B., Spencer, J. & Wormald, N. Sudden emergence of a giant *k*-core in a random graph. *J. Comb. Theory B* **67,** 111–151 (1996).
34. Nagler, J., Levina, A. & Timme, M. Impact of single links in competitive percolation. *Nature Phys.* **7,** 265–270 (2011).
35. Bianconi, G. & Dorogovtsev, S. N. Percolation in networks of networks with random matching of nodes in different layers. Preprint at http://arXiv.org/abs/1411.4160 (2014).
36. Stark, C. *et al.* Biogrid: A general repository for interaction datasets. *Nucleic Acids Res.* **34,** D535–D539 (2006).
37. De Domenico, M., Porter, M. A. & Arenas, A. Muxviz: A tool for multilayer analysis and visualization of networks. *J. Complex Netw.* **3,** 159–176 (2015).
38. Guimerà, R., Mossa, S., Turtschi, A. & Amaral, L. N. The worldwide air transportation network: Anomalous centrality, community structure, and cities' global roles. *Proc. Natl Acad. Sci. USA* **102,** 7794–7799 (2005).
39. Colizza, V., Barrat, A., Barthélemy, M. & Vespignani, A. The role of the airline transportation network in the prediction and predictability of global epidemics. *Proc. Natl Acad. Sci. USA* **103,** 2015–2020 (2006).
40. *TranStats* (United States Department of Transportation, accessed 18 January 2015); http://www.transtats.bts.gov

Acknowledgements

The author thanks C. Castellano and A. Flammini for comments and suggestions.

Additional information

Supplementary information is available in the online version of the paper. Reprints and permissions information is available online at www.nature.com/reprints.

Competing financial interests

The author declares no competing financial interests.